Egyptian Journal of Radiology and Nuclear Medicine

RESEARCH

Open Access

Differentiating multiple sclerosis from cerebral small vessel disease using diffusion tensor imaging and magnetic resonance spectroscopy on normally appearing thalami

Sahar Mahmoud Abd elsalam[1], Soheir Salah[1], Ahmed Hesham Said[1], Mona Hussein[2], Rehab Magdy[3] and Wesam Osama[3*]

Abstract

Background Diffusion tensor imaging (DTI) and magnetic resonance spectroscopy (1H-MRS) can detect the microstructural changes in normal-appearing conventional MRI. So, they may differentiate between multiple sclerosis (MS) cases and cerebral small vessel disease (CSVD). This work aimed to investigate if MRS and DTI are helpful in differentiating between MS and CSVD cases.

Methods The study was conducted on 90 subjects divided into three groups: 30 relapsing–remitting MS patients, 30 patients with MRI showing CSVD, and 30 healthy controls. Diffusion tensor imaging measuring thalamic FA, ADC values, and 1H-MRS were conducted on patients and controls.

Results Thalamic FA values were significantly higher in the RRMS group than in the control and CSVD groups ($P < 0.001$, for each) but significantly lower in the CSVD group than the control group ($P < 0.001$). Moreover, thalamic ADC values were significantly higher in the CSVD group than in the control and MS groups ($P < 0.001$, for each). Also, thalamic NAA values were significantly lower in RRMS and CSVD groups than in controls ($P < 0.001$ for each). Still, they were significantly lower in the RRMS group than the CSVD group only on the left side ($P = 0.004$). The thalamic NAA/Cr values were significantly lower in RRMS ($P < 0.001$ for both sides) and CVSD than in controls ($P = 0.044$ and 0.036, for RT and LT sides, respectively).

Conclusions Thalamic DTI and 1H-MRS can help detect the microstructural changes in normal-appearing thalami in RRMS and CSVD patients. Moreover, they can help differentiate MS from CSVD patients.

Keywords DTI, 1H-MRS, Multiple sclerosis, Cerebral small vessel disease, Thalami, Grey matter

*Correspondence:
Wesam Osama
wesamosama9@yahoo.com
[1] Department of Radiology, Faculty of Medicine, Beni-Suef University, Beni-Suef, Egypt
[2] Department of Neurology, Faculty of Medicine, Beni-Suef University, Beni-Suef, Egypt
[3] Department of Neurology, Faculty of Medicine, Cairo University, Cairo, Egypt

Background

White matter lesions of multiple sclerosis (MS) and cerebral small vessel disease (CSVD) may appear similarly on conventional MRI as both cause hyperintense lesions on T2 images [1]. Cerebral small vessel disease is a condition resulting from damage to the cerebral microcirculation. It predominantly affects the brain's deep white and grey

matter areas [2]. Also, both white and grey matter can be involved in MS [3].

Conventional MRI cannot accurately detect the microstructural changes in normal-appearing white and grey matter. Diffusion tensor imaging (DTI) and magnetic resonance spectroscopy (1H-MRS) are sensitive to these changes [4–6]. Magnetic resonance spectroscopy helps as a noninvasive technique for detecting and quantifying metabolite concentrations in the brain, providing a chemical-pathological characterization of MR visible lesions and normal-appearing white and grey matter [7]. Also, DTI parameters, including fractional anisotropy (FA) and apparent diffusion coefficient (ADC), show high sensitivity to occult damage of brain tissues in both grey and white matter [8].

Thalamus is a grey matter structure that has well-defined boundaries. The thalamus also has extensive connections with the cortex and subcortical structures, so it is likely to be sensitive to the effects of pathology in many brain areas [9].

Differentiation between white matter lesions caused by MS and those caused by CSVD on conventional brain MRI may not always be accessible in equivocal cases. Although age is a helpful parameter, it may be misleading. Multiple sclerosis is primarily a disease of young adults; however, it may affect all ages. Cerebral small vessel disease is more frequently seen in old age, but up to 20% of patients are below 50 years old, so the occurrence of these diseases in the same age group is not rare [1]. Failure to correctly identify and diagnose the two diseases may delay early intervention, affecting their prognosis [10]. This study aimed to investigate if MRS and DTI are helpful in differentiating between MS and CSVD cases.

Methods

This case–control study was conducted on 90 subjects divided into three groups: 30 patients diagnosed with RRMS (during remission), 30 patients with MRI showing CSVD, and 30 healthy controls. The age of RRMS patients in this study ranged from 20 to 50 years with a mean value of 35.3 ± 9 years, of CSVD patients ranged from 49 to 70 with a mean value of 57 ± 6 years and in the healthy control group ranged from 21 to 61 with a mean value of 37 ± 11.3 years. Regarding gender distribution, 66.7% ($n=20$) were females, and 33.3% ($n=10$) were males in the RRMS group, 43.3% ($n=13$) were females, and 56.7% ($n=17$) were males in the CSVD group, while 56.7% ($n=17$) females and 43.3% ($n=13$) males consisted the control group.

The patients were selected from our clinic at our University Hospital. Written informed consent was obtained from each participant in this study.

Patients who fulfill "McDonald's criteria 2017" for the diagnosis of RRMS [11] should be in remission (at least three months from the last relapse) and have no evidence of vascular comorbidity with normal-appearing thalami on conventional MRI.

Patients with vascular risk factors such as hypertension, diabetes mellitus, and dyslipidemia with multiple hyperintense foci in the cerebral WM on conventional T2-weighted and FLAIR MR images with normal-appearing thalami were recruited as the CSVD group. Patients with clinical/laboratory findings suggestive of non-vascular etiology of white matter lesions like associated autoimmune disease, hematological disorder, malignancy, CNS inflammatory or infectious disorder, or traumatic brain injury were excluded. The eligibility flowchart of patients' selection is shown in (Fig. 1).

Healthy volunteers with no evidence of vascular risk factors such as hypertension, diabetes mellitus, dyslipidemia, a history of smoking, or autoimmune disorders were recruited as the control group. All had normal findings on conventional MRI.

All study groups were submitted to thorough history taking and neurological examination included MS patients were further evaluated by the Expanded Disability Status Scale (EDSS) [12].

All MR Images were analyzed by two experienced radiologists with 25 and 20 years of experience in neuroimaging. Image interpretation and final reports were written in consensus. For each group (Ms and CSVD), a definite diagnosis has been made clinically and radiologically for all patients. Likewise, two neurologists evaluated each patient with at least 15 years of experience.

Image acquisition and interpretation

Magnetic resonance imaging (MRI)

MRI brain performed for all included patients and controls by a 1.5 Tesla Siemens scanner, Germany, with the following routine sequences used: T1WI (axial, sagittal), T2WI (axial, coronal), and FLAIR (axial) as well as axial DWI SE/EPI sequence. To confirm the absence of abnormal signals within the thalami, T2 & FLAIR images were reviewed.

Diffusion tensor imaging (DTI)

Diffusion tensor imaging was performed using spin-echo /echo-planar imaging (SE/EPI) sequence along 20 different diffusion-encoding directions with two b values for each direction 0 and 1000 s/mm2, with technical parameters as follows: TR/TE 6200/142 ms, FOV 248 × 248 mm, matrix 128 × 128, 5 mm slice thickness with no gap, number of averages 3, the acquisition time was 6:51 min.

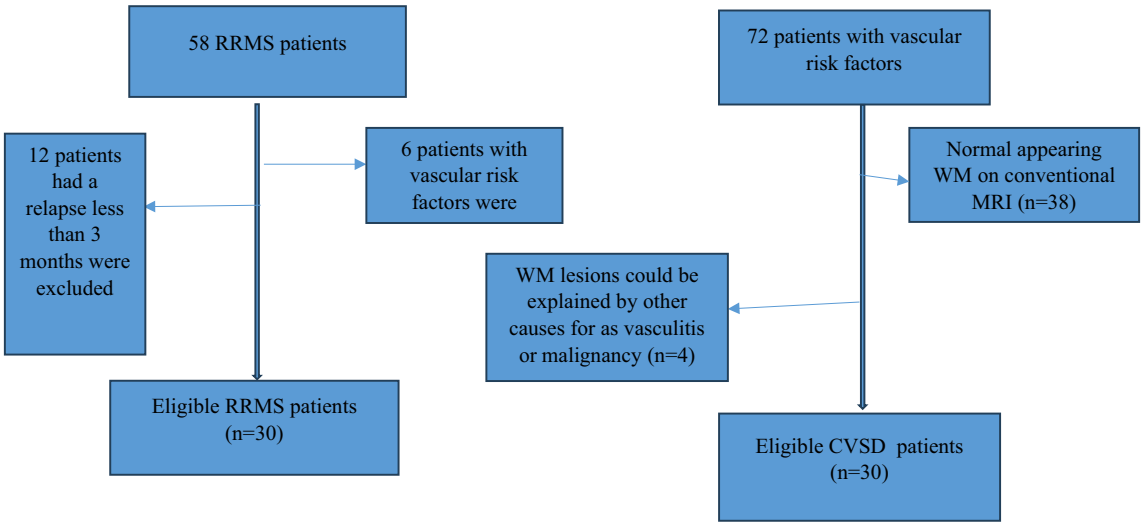

Fig. 1 Flowchart for the eligibility criteria of included patients

Proton magnetic resonance spectroscopy (MRS)

2D multi-voxel 1H-MRS scanning with short TE was performed with a chemical shift imaging PRESS sequence was used for VOI selection. The sequence parameters were, TR/TE = 1500 /35 ms, FOV = 160 × 160 mm, volume of interest 80 × 80 mm and 4 preparation scans, bandwidth 1000 Hz, vector size 1024 and voxel size 10 × 10x15 mm.

Image analysis

All MR images were analysed by two experienced radiologists with 25 and 20 years of experience in neuroimaging. Image interpretation and final report were written in consensus with qualitative and quantitative analyses of the images.

Qualitative assessment for the distribution, number and characteristic features of the white matter lesions, the right and left thalami were reviewed in both T2 & FLAIR images to confirm the absence of abnormal signals within.

Quantitative assessment

DTI

Automatic reconstruction of B_o images, apparent diffusion coefficient (ADC), and fractional anisotropy (FA) maps from the echo planar diffusion images were done on manufacturer software. Standard circular ROIs with an area of 0.50 ± 0.01cm2 were selected from the central portions of the thalami far away enough from the ventricles medially and internal capsules laterally to avoid contamination of these tissues, FA and ADC were generated for each thalamus.

Proton magnetic resonance spectroscopy (MRS)

Quantification of the spectra was performed from both thalami by selecting voxels away from the lateral ventricles medially and internal capsules laterally with spectra for (N-acetyl aspartate (NAA) at 2.03 ppm, Creatine (Cr) at 3.04 ppm, Choline (Cho) at 3.22 ppm, Myo-inositol at 3.56 ppm. Also, NAA/Cr and NAA/Cho ratios were calculated.

Ethical statement

The study was approved by the ethical committee in the Faculty of Medicine, our University (Approval number: FMBSUREC/03012021/Mohamed). Written informed consent was obtained from each participant in this study.

Statistical analysis

The data were coded and entered using the Statistical Package for Social Science version 20 (SPSSv 20). The data were summarized using mean and standard deviation for quantitative data and the frequency distribution for qualitative data. Student *t*-test was used to compare the means of two groups of quantitative variables. The *P*-value is significant if < 0.05.

Results

The clinical characteristics of RRMS and CVSD groups are illustrated in Tables 1 and 2.

Table 1 Clinical characteristics of the included RRMS patients

		RRMS group ($n=30$)
Disease duration [mean ± SD]		5.53 ± 3.85
Total number of relapses [mean ± SD]		2.27 ± 1.16
EDSS [mean ± SD]		1.86 ± 1.26
DMDs	Yes	24 (80%)
	No	6 (20%)

RRMS Relapsing–remitting multiple sclerosis, *SD* Standard deviation, *DMDs* Disease-modifying Drugs, *EDSS* Expanded disability status scale

Table 2 Clinical characteristics of the patients with CSVD

		Patients with CSVD ($n=30$)
Hypertension	Yes [*n* (%)]	24 (80%)
	No [*n* (%)]	6 (20%)
Diabetes Mellitus	Yes [*n* (%)]	16 (53.3%)
	No [*n* (%)]	14 (46.7%)
Smoking	Yes [*n* (%)]	15 (50%)
	No [*n* (%)]	15 (50%)
AF	Yes [*n* (%)]	1 (3.3%)
	No [*n* (%)]	29 (96.7%)

CSVD Cerebral small vessel disease, *AF* Atrial fibrillation

Diffusion tensor imaging parameters (DTI) findings

Regarding both thalamic FA mean values, there was a statistically significant difference between the RRMS and the control group, being significantly higher in the RRMS group (*P*-value < 0.001). There was also a statistically significant difference between the CSVD and the control group, being significantly lower in the CSVD group (*P*-value < 0.001). A statistically significant difference was also found between the RRMS and CSVD groups (*P*-value < 0.001) (Table 3).

There was no statistically significant difference between the RRMS and the control group for the right and left thalamic mean ADC values. On the other hand, both thalamic ADC mean values were significantly higher in the CSVD group than in the control group (*P*-value < 0.001). Also, both thalamic ADC mean values were significantly higher in the CSVD group than in the RRMS group (*P*-value < 0.001) (Table 3).

Magnetic resonance spectroscopy (MRS) metabolites

The thalamic NAA mean value was significantly lower in the RRMS group than in the CVSD group, only on the left side. Also, thalamic NAA mean values (RT and LT) were significantly lower in both RRMS and CVSD groups than in controls (Table 4).

However, there was no statistically significant difference between the three study groups regarding right and left thalamic mean choline, creatine, and myoinositol values.

The thalamic NAA/Cr mean values (RT and LT) were significantly lower in both RRMS and CVSD groups than in controls. However, there was no statistically significant difference between RRMS and CVSD groups (Table 4).

In addition, the RT thalamic NAA /Cho mean value was significantly lower in both RRMS and CVSD groups than in controls. In contrast, the LT thalamic NAA /Cho mean value was significantly lower in the RRMS group than in CVSD and control groups (Table 4).

Cut-off points of MRI parameters in the detection of RRMS and CVSD

Roc curve analysis revealed that the best discrimination between RRMS and controls was achieved at the LT FA cut-off of 280 (AUC = 0.888), followed by the LT NAA/Cho cut-off of 2.48 (AUC = 0.775) (Table 5). For the right side, the FA cut-off of 276 (AUC = 0.858), followed by the NAA/Cho cut-off of 9.35 (AUC = 0.849) were the best (Table 6).

Also, the best discrimination between CVSD and controls was achieved at the LT ADC cut-off of 786 (AUC = 0.992), followed by LT FA at 255 (AUC = 0.823), then the LT NAA cut-off of 9.24 (AUC = 0.777) (Table 7). For the right side, the ADC cut-off of 785 (AUC = 0.987),

Table 3 Diffusion tensor imaging findings in the included patients and control groups

		RRMS group ($n=30$) [mean ± SD]	CSVD group ($n=30$) [mean ± SD]	Control group ($n=30$) [mean ± SD]	RRMS vs. CSVD *P*-value	RRMS vs. controls *P*-value	CSVD vs. controls *P*-value
FA	Rt	297.8 ± 16.9	237.2 ± 20.3	268.7 ± 21.7	< 0.001*	< 0.001*	< 0.001*
	Lt	297.6 ± 18.3	234.1 ± 25.3	262.8 ± 22.4	< 0.001*	< 0.001*	< 0.001*
ADC	Rt	747.9 ± 18.9	881.7 ± 127.6	745.8 ± 23	< 0.001*	0.913	< 0.001*
	Lt	746.5 ± 17.9	879.7 ± 115.6	746.3 ± 22.3	< 0.001*	0.995	< 0.001*

*P value is considered significant at ≥ 0.05

FA Fractional anisotropy, *ADC* Apparent diffusion coefficient, *RRMS* Relapsing–remitting multiple sclerosis, *CSVD* Cerebral small vessel disease, *SD* Standard deviation

A *P*-value < 0.05 is considered significant

Table 4 Magnetic resonance spectroscopy findings in the included patients and control groups

		RRMS group ($n=30$) [mean ± SD]	CSVD group ($n=30$) [mean ± SD]	Control group ($n=30$) [mean ± SD]	RRMS vs. CSVD *P*-value	RRMS vs. controls *P*-value	CSVD vs. controls *P*-value
NAA	Rt	8.5 ± 1.18	9.1 ± 1.1	10.3 ± 1.3	0.078	< 0.001*	< 0.001*
	Lt	8.2 ± 1	9 ± 1.1	10.2 ± 1.1	0.004*	< 0.001*	< 0.001*
Cr	Rt	5 ± 0 .6	4.9 ± 0.5	5.1 ± 0.6	0.280	0.893	0.225
	Lt	4.9 ± 0.6	5 ± 0.65	5.1 ± 0.5	0.403	0.111	0.442
Cho	Rt	4 ± 0.7	3.8 ± 0.6	3.9 ± 0.8	0.379	0.639	0.680
	Lt	4.1 ± 0.66	3.7 ± 0.8	4 ± 0.85	0.090	0.699	0.188
NAA/Cr	Rt	1.7 ± 0.35	1.9 ± 0.3	2 ± 0.3	0.087	< 0.001*	0.044*
	Lt	1.7 ± 0.3	1.8 ± 0.3	2 ± 0.35	0.182	0.001*	0.036*
NAA /Cho	Rt	2.2 ± 0.6	2.4 ± 0.4	2.7 ± 0.7	0.322	0.001*	0.018*
	Lt	2.1 ± 0.44	2.5 ± 0.5	2.7 ± 0.8	0.011*	< 0.001*	0.239
MI	Rt	1.4 ± 0.45	1.5 ± 0.35	1.3 ± 0.56	0.332	0.566	0.124
	Lt	1.5 ± 0.37	1.5 ± 0.4	1.4 ± 0.4	0.530	0.238	0.072

*P value is considered significant at ≥ 0.05

Cho Choline, *Cr* Creatine, *MI* Myo-inositol, *NAA* N-Acetyl aspartate, *RRMS* Relapsing–remitting multiple sclerosis, *CSVD* Cerebral small vessel disease, *SD* Standard deviation

A *P*-value < 0.05 is considered significant

Table 5 Cut-off, sensitivity, specificity, positive predictive value, and negative predictive value of MRI parameters (on the left side) in the detection of RRMS (compared with controls)

	LT FA	LT ADC	LT NAA	LT NAA/Cho	LT NAA/Cr
Cut off	> 280	≤ 740	≤ 9.01	≤ 2.48	≤ 1.82
P-value	< 0.001*	0.767	< 0.001*	< 0.001*	< 0.001*
AUC	0.888	0.523	0.897	0.775	0.761
Sensitivity (95% CI)	83.33 (65.3–94.4)	50.0 (31.3–68.7)	86.6 (69.3–96.2)	86.67 (69.3–96.2)	66.6 (47.2–82.7)
Specificity (95% CI)	90.0 (73.5–97.9)	66.67 (47.2–82.7)	86.6 (69.3–96.2)	56.6 (37.4–74.5)	66.67 (47.2–82.7)
PPV (95% CI)	89.3 (73.8–96.1)	60.0 (44.7–73.6)	86.7 (72.1–94.2)	66.7 (56.5–75.5)	66.7 (53.2–77.9)
NPV (95% CI)	84.4 (70.6–92.4)	57.1 (46.2–67.4)	86.7 (72.1–94.2)	81.0 (61.8–91.8)	66.7 (53.2–77.9)

*P value is considered significant at ≥ 0.05

AUC Area under the curve, *PPV* Positive predictive value, *NPV* Negative predictive value, *CI* Confidence interval

Table 6 Cut off, sensitivity, specificity, positive predictive value, and negative predictive value of MRI parameters (on the Rt side) in the detection of RRMS (compared with controls)

	RT FA	RT ADC	RT NAA	RT NAA/Cho	RT NAA/Cr
Cut off	> 276	≤ 756	≤ 9.35	≤ 2.3	≤ 1.77
P-value	< 0.001*	0983	< 0.001*	< 0.001*	< 0.001*
AUC	0.858	0.502	0.849	0.749	0.771
Sensitivity (95% CI)	96.6 (82.8–99.9)	76.67 (57.7–90.1)	80.0 (61.4–92.3)	66.6 (47.2–82.7)	63.3 (43.9–80.1)
Specificity (95% CI)	76.67 (57.7–90.1)	33.3 (17.3–52.8)	76.6 (57.7–90.1)	60.0 (40.6–77.3)	86.67 (69.3–96.2)
PPV (95% CI)	80.6 (68.3–88.8)	53.5 (45.5–61.3)	77.4 (63.6–87.0)	62.5 (50.1–73.4)	82.6 (64.7–92.5)
NPV (95% CI)	95.8 (76.8–99.4)	58.8 (38.6–76.5)	79.3 (64.6–89.0)	64.3 (50.1–76.4)	70.3 (59.1–79.4)

*P value is considered significant at ≥ 0.05

AUC Area under the curve, *PPV* Positive predictive value, *NPV* Negative predictive value, *CI* Confidence interval

Table 7 Cut off, sensitivity, specificity, positive predictive value, and negative predictive value of MRI parameters (on the left side) in the detection of CSVD (compared with controls)

	LT FA	LT ADC	LT NAA	LT NAA/Cho	LT NAA/Cr
Cut off	≤ 255	> 786	≤ 9.24	≤ 2.8	≤ 1.86
P-value	< 0.001*	< 0.001*	< 0.001*	0.540	0.024*
AUC	0.823	0.992	0.777	0.593	0.659
Sensitivity (95% CI)	80.0 (61.4–92.3)	93.3 (77.9–99.2)	70.0 (50.6–85.3)	76.6 (57.7–90.1)	56.6 (37.4–74.5)
Specificity (95% CI)	73.3 (54.1–87.7)	100.0 (88.4–100.0)	86.6 (69.3–96.2)	40.0 (22.7–59.4)	56.6 (37.4–74.5)
PPV (95% CI)	75.0 (61.7–84.8)	199 (85–100)	84.0 (67.2–93.1)	56.1 (47.3–64.5)	56.7 (43.9–68.6)
NPV (95% CI)	78.6 (63.5–88.6)	93.7 (79.7 -98.3)	74.3 (62.2–83.6)	63.2 (43.9–78.9)	56.7 (43.9–68.6)

*P value is considered significant at ≥ 0.05

AUC Area under the curve, *PPV* Positive predictive value, *NPV* Negative predictive value, *CI* Confidence interval

Table 8 Cut off, sensitivity, specificity, positive predictive value, and negative predictive value of MRI parameters (on the Rt side) in detection of CSVD disease (compared with controls)

	RT FA	RT ADC	RT NAA	RT NAA/Cho	RT NAA/Cr
Cut off	≤ 253	> 785	≤ 9.86	≤ 2.9	≤ 2
P-value	< 0.001*	< 0.001*	< 0.001*	0.040*	0.009*
AUC	0.879	0.987	0.763	0.647	0.680
Sensitivity (95% CI)	86.67 (69.3(96.2)	90.0 (73.5–97.9)	86.6 (69.3–96.2)	90.0 (73.5–97.9)	83.3 (65.3–94.4)
Specificity (95% CI)	80.0 (61.4–92.3)	100.0 (88.4–100.0)	60.0 (40.6–77.3)	36.6 (19.9–56.1)	46.6 (28.3–65.7)
PPV (95% CI)	81.2 (67.6–90.0)	100.0 (88.4–100.0)	68.4 (57.8–77.4)	58.7(51.4–65.7	61.0 (51.9—69.4)
NPV (95% CI)	85.7 (70.3–93.8)	90.9 (77.4–96.7)	81.8 (63.3–92.1)	78.6 (53.2–92.2)	73.7 (53.6–87.2)

*P value is considered significant at ≥ 0.05

AUC Area under the curve, *PPV* Positive predictive value, *NPV* Negative predictive value, *CI* confidence interval

followed by FA at 253 (AUC = 0.879), then the NAA cut-off of 9.86 (AUC = 0.763) (Table 8).

Neuroimaging of different cases is illustrated in Figs. (2, 3, 4, 5, 6, 7, 8 and 9).

Discussion

White matter lesions of MS and CSVD may appear similarly on conventional MRI [13]. Diffusion tensor imaging (DTI) and 1H-MRS can detect the microstructural changes in normal-appearing conventional MRI [1]. Accordingly, this study aimed to investigate if 1H-MRS and DTI measures on normally appearing thalami are helpful in differentiating between MS and CSVD cases.

The current study highlighted the excellent distinctive performance of thalamic DTI measures in differentiating between RRMS and CSVD groups and each of them from the control group. Thalamic FA was significantly increased in RRMS patients and decreased in CSVD patients compared to the control group ($P < 0.001$). In the same time, its value was significantly higher in the RRMS than CSVD groups. Moreover, thalamic ADC was significantly higher in CSVD patients compared to RRMS patients and the control group.

These results aligned with previous studies [14–16], which found a significantly higher thalamic FA in

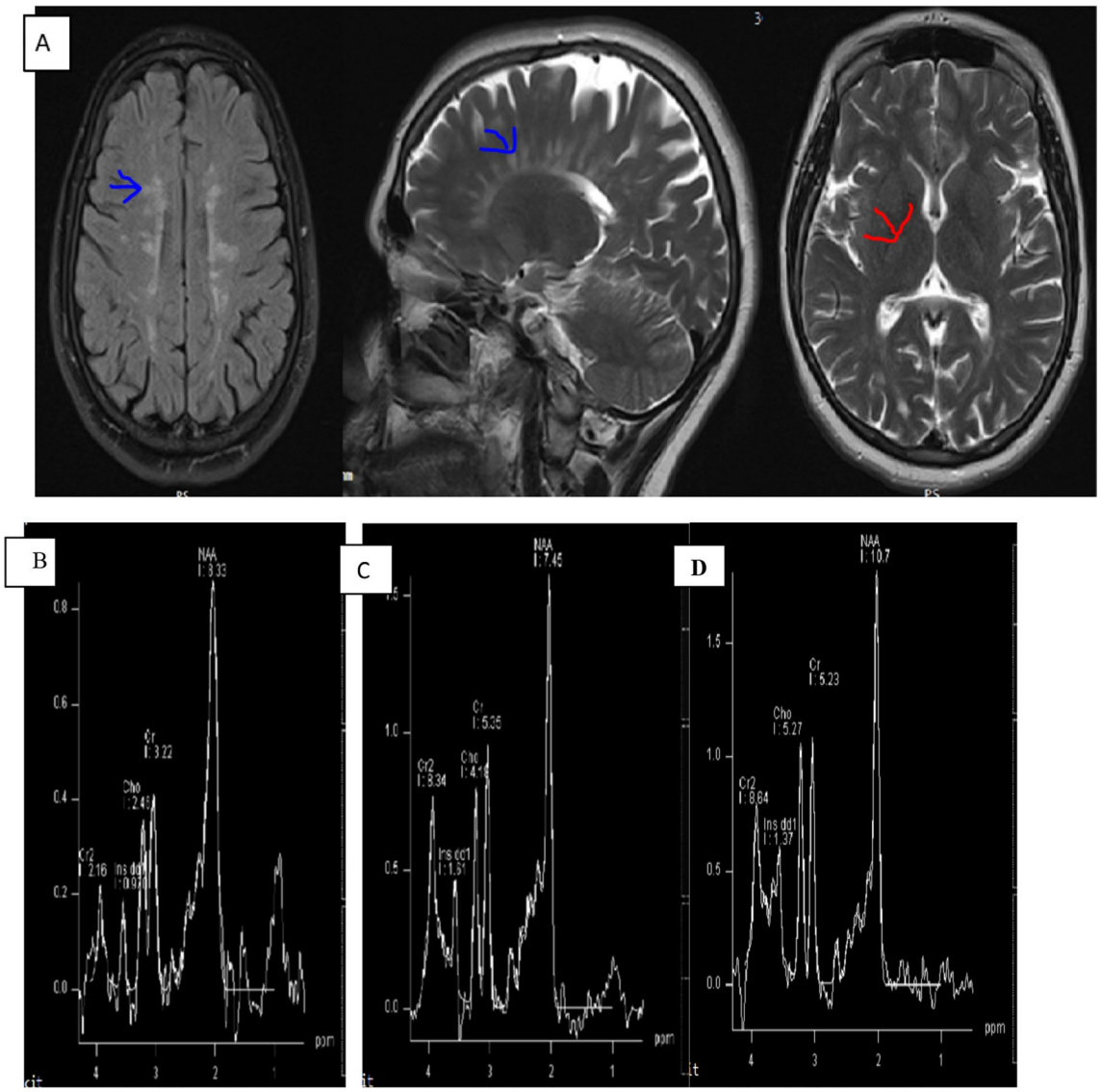

Fig. 2 A 37-year-old female patient complaining of RRMS, image **A** (axial FLAIR, sagittal and axial T2) showing ovoid-shaped periventricular T2 / FLAIR hyperintense lesions being perpendicular on lateral ventricular wall (blue arrow), with axial T2 WIs showing normal appearing thalami (red arrow). Right thalamic MRS, NAA value = 8.3 Mm (**B**), Left thalamic NAA value = 7.5 Mm (**C**), compared to control NAA value 10.7 Mm (**D**)

MS cases than controls. This can be explained by the fact that anisotropy was correlated to axon density and myelin content, which are affected by pathologic abnormalities occurring in MS as a result of dendritic loss and bipolar orientation caused by microglial activation and extra axonal degeneration in grey matter nuclei [17, 18].

In agreement with the current work, Öztoprak et al. [19] found that the mean ADC value was significantly higher in patients with CSVD compared to MS patients and controls and that FA value was significantly less in CSVD cases than controls. The high ADC values in CSVD can be explained by the fact that the infracted brain tissues liquidize, so their molecules have free

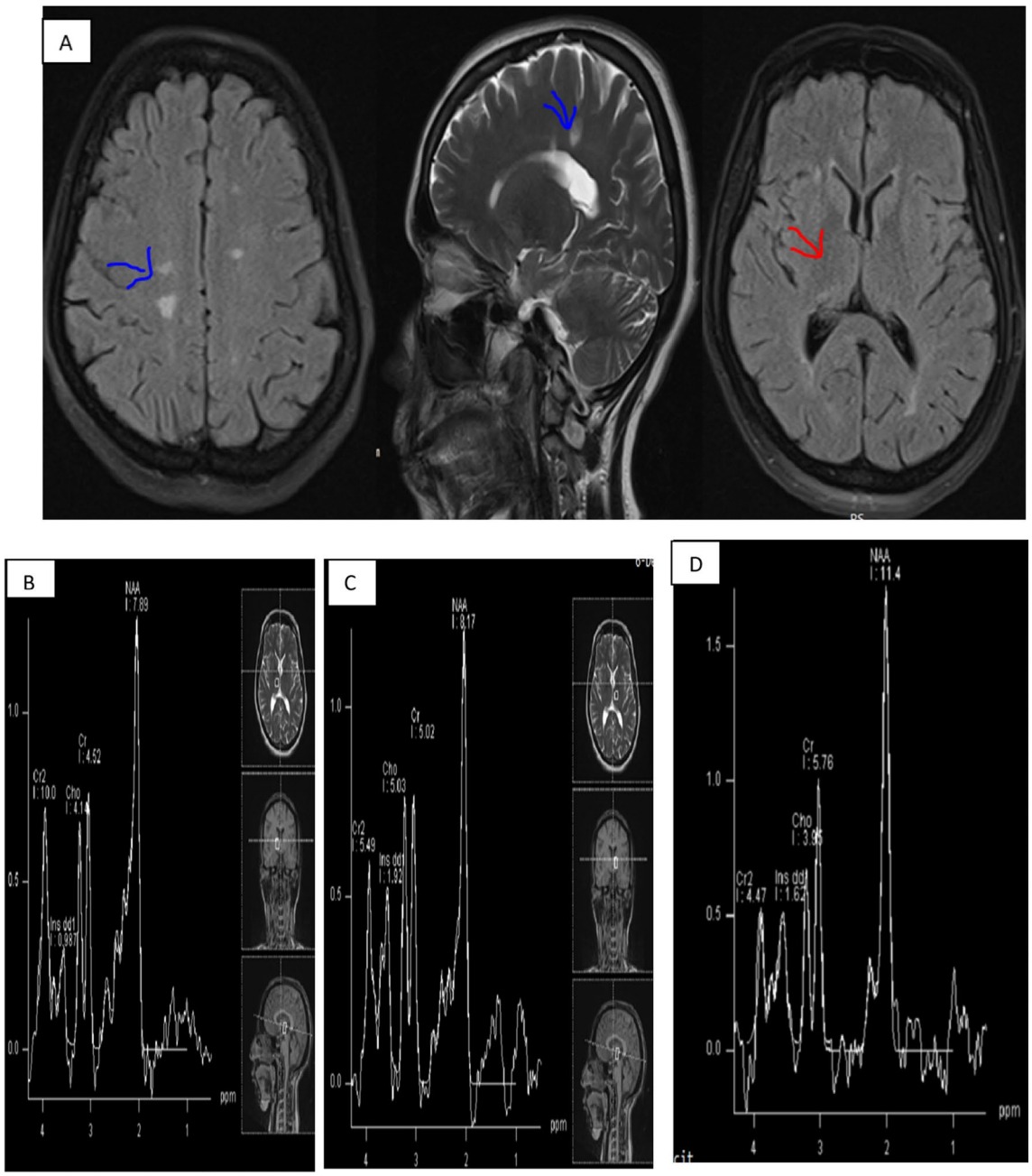

Fig. 3 A 38-year-old female patient complaining of RRMS, image **A** (axial FLAIR, sagittal T2 and axial FLAIR) showing ovoid shaped periventricular T2 /FLAIR hyperintense lesions (blue arrow) and normal appearing thalami (red arrow), Right thalamic MRS, NAA value 7.9 Mm **B**, Left thalamic NAA value 8.2 Mm **C**, compared to control thalamic NAA value 11.4 Mm (**D**)

movement and high ADC value compared to normal brain tissues [20].

By studying the neuronal metabolites provided by MRS, this study showed that MRS could aid in differentiation between either RRMS or CSVD and the control group. However, it could not firmly discriminate between MS and CSVD groups. This evident by lower bilateral thalamic NAA, NAA/Cr, and right NAA/Cho mean values in both RRMS and CSVD groups than in the control group, with no statistically significant difference between

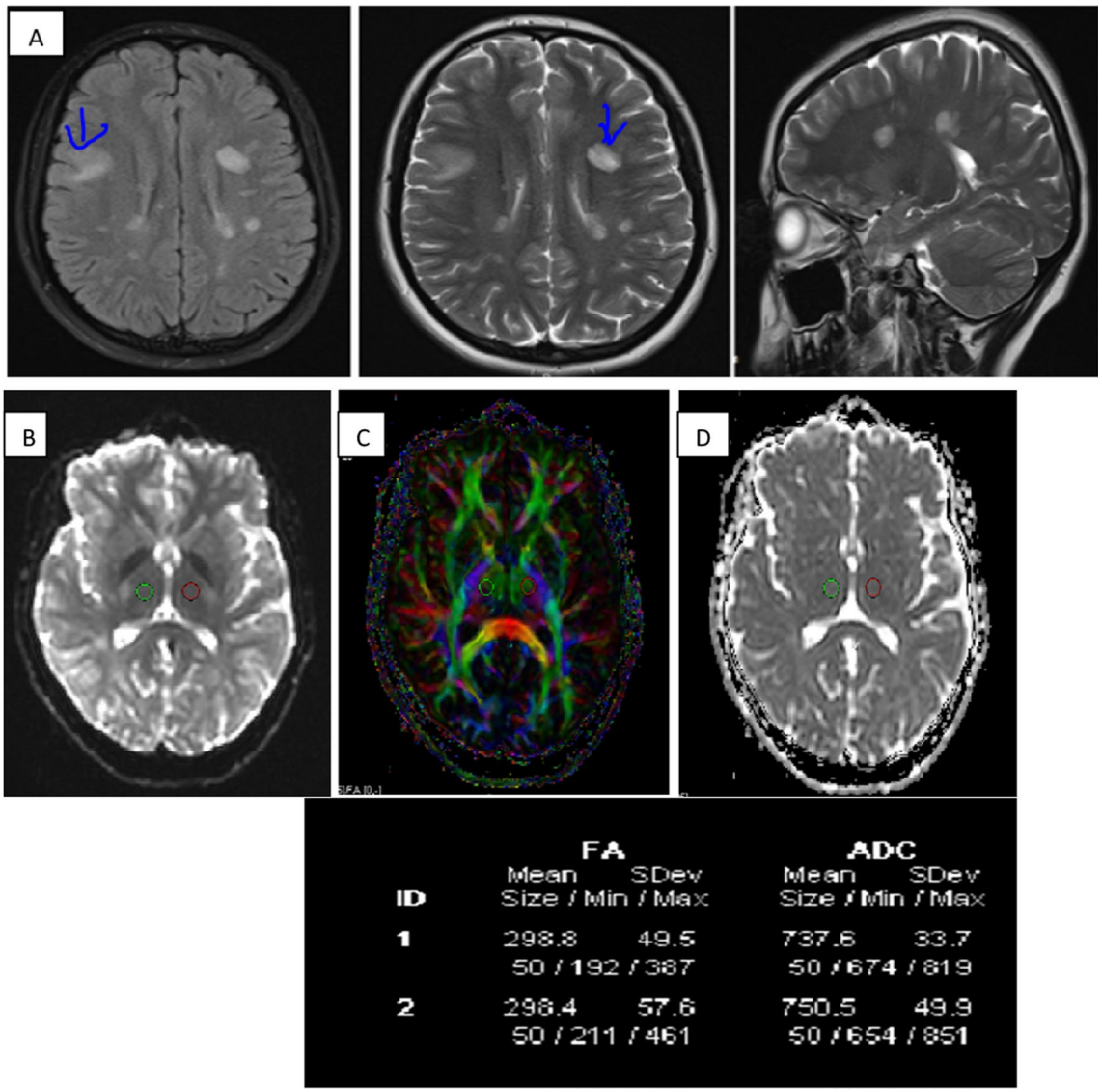

Fig. 4 A 30-year-old female patient complaining of RRMS, image **A** (axial FLAIR, axial and sagittal T2) showing ovoid shaped periventricular & cortical/juxtacortical T2 /FLAIR hyperintense lesions (blue arrow) with normal appearing thalami. ROI placement in DTI B0 images **B**, colored FA images **C** and ADC images **D**. The table below shows thalamic FA value of 298 for the right and 299 for the left, ADC value 751×10^{-6} mm^2/s for the right thalamus and 738×10^{-6} mm^2/s for the left one

the RRMS and CSVD groups as regards the previously mentioned regions.

Reduced NAA concentration is mainly inferred as neuronal/axonal dysfunction that can happen both in MS and CSVD patients [21, 22]. Notably, NAA decline without concomitant Cr increase might indicate initial neuronal loss without a significant involvement with glial cells [23]. Regarding CSVD patients, it has been found that thrombin inhibition improves the NAA/Cr ratio, suggesting that arterial thrombosis may have a role in the development of metabolic impairment of neurons [24].

The thalamus was also submitted to MRS analysis in a group of MS patients by Geurts et al. [25]. The

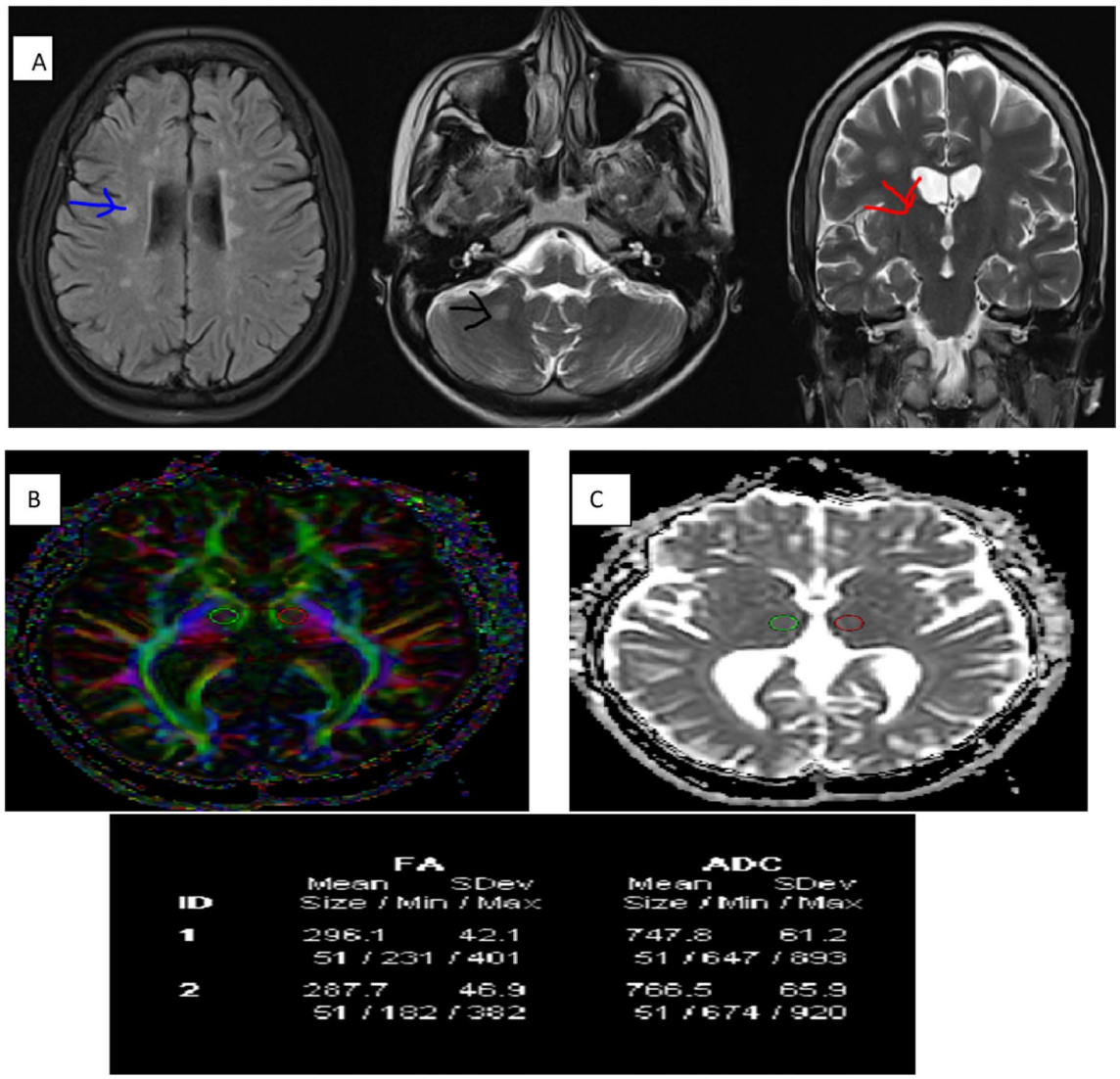

Fig. 5 A 42-year-old male patient complaining of RRMS, image **A** (axial FLAIR, axial and coronal T2) showing periventricular white matter (blue arrow) & bilateral middle cerebellar peduncles (black arrow)T2 /FLAIR hyperintense lesions and normal appearing thalami (red arrow). Thalamic DTI ROI placement in colored FA images **B** and ADC images **C**. The table below shows thalamic FA value of 288 for the right and 296 for the left, ADC value 766 × 10–6 mm2/s for the right thalamus and 748 × 10–6 mm2/s for the left one

investigators found a significant reduction in NAA values in MS patients than the healthy controls with no significant differences regarding creatinine or choline values; all are concordant with the current study.

Another study carried out by Kapeller et al. [26] investigated the potential role of MRS in differentiating MS plaques from CSVD. They found a significant increase in the myoinositol concentrations in MS plaques than white matter lesions in CSVD, with no significant differences regarding the other metabolites. However, studying the thalamic metabolic alterations as a distinguishing radiological marker between MS and CSVD has not been conducted before.

The main limitation of this study was that the number and sites of either MS or CSVD lesions wasn't considered. Moreover, this study used a 1.5 T MRI scanner, while most cited studies used 3 T. The small sample size was also another critical limitation.

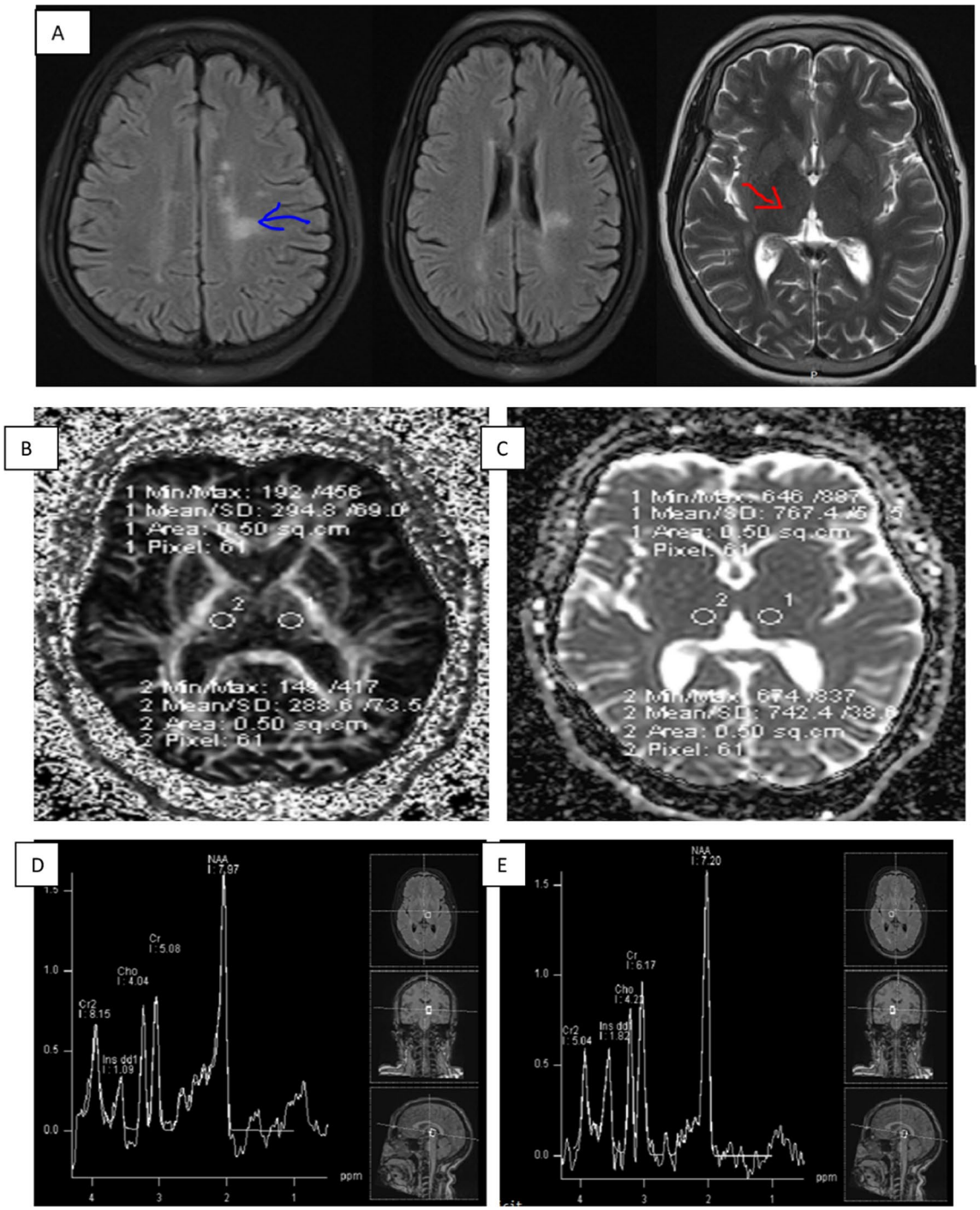

Fig. 6 A 28-year-old female patient complaining of RRMS, image **A** (axial FLAIR, axial T2) showing periventricular T2 /FLAIR hyper intense lesions more evident at left side (blue arrow) and normal appearing thalami (red arrow). ROI placement in FA images with thalamic value of 288 for the right and 295 for the left one (**B**), ROI placement in ADC images with thalamic value of 742×10^{-6} mm^2/s for the right and 767×10^{-6} mm^2/s for the left one (**C**). Right thalamic MR spectra, NAA value = 7.2 Mm (**D**), Left thalamic MR spectra, NAA = 7.9 Mm (**E**)

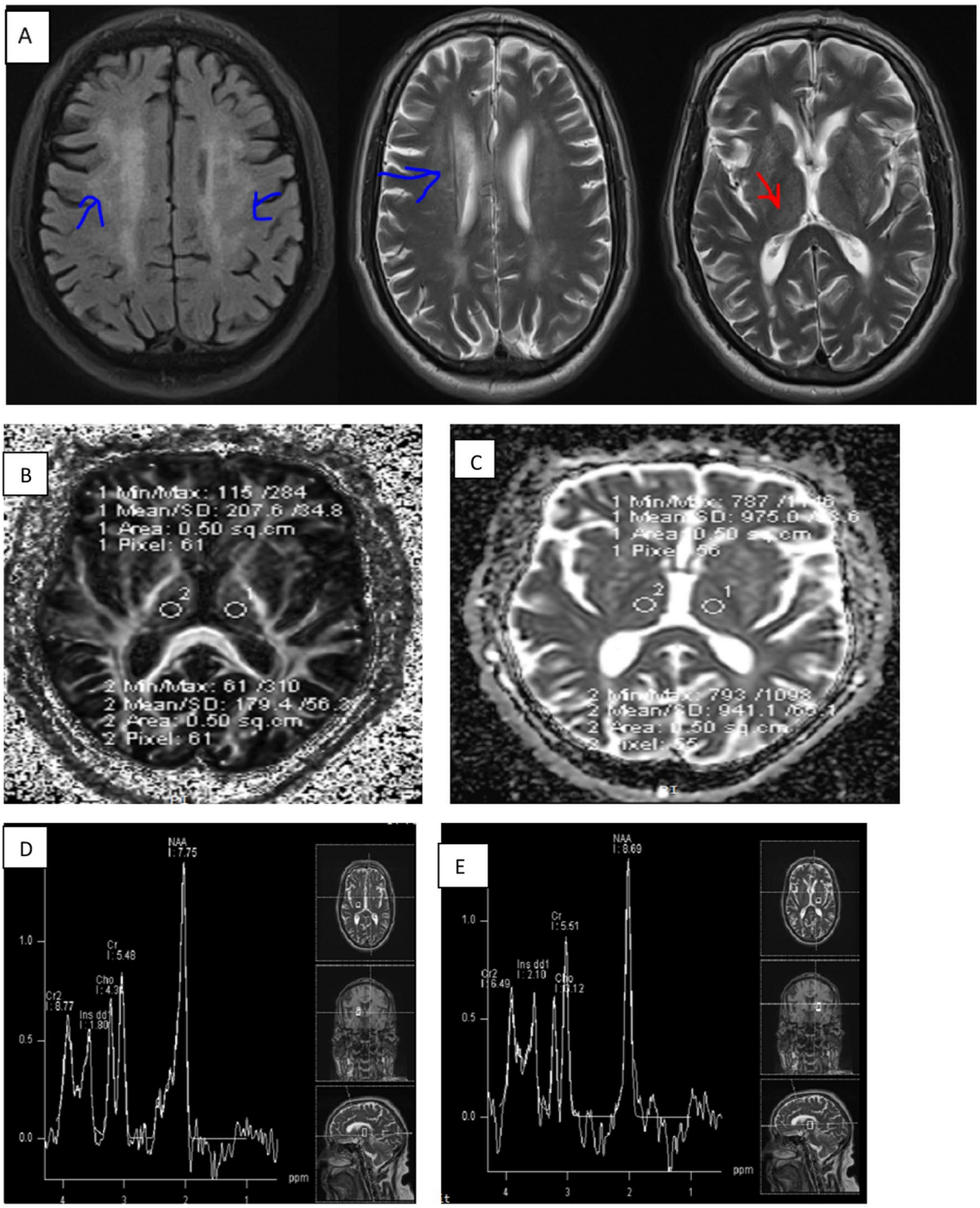

Fig. 7 A 60-year-old male patient complaining of CSVD, image **A** (axial FLAIR and axial T2) showing periventricular T2 /FLAIR hyper intense lesions (blue arrow) and normal appearing thalami (red arrow). ROI placement in FA images with thalamic value of 179 for the right and 207 for the left one (**B**), ROI placement in ADC images with thalamic value of 941×10^{-6} mm^2/s for the right and 975×10^{-6} mm^2/s for the left one (**C**). Right thalamic MR spectra NAA value = 7.8 Mm (**D**), Left thalamic MR spectra, NAA = 7.9 Mm (**E**)

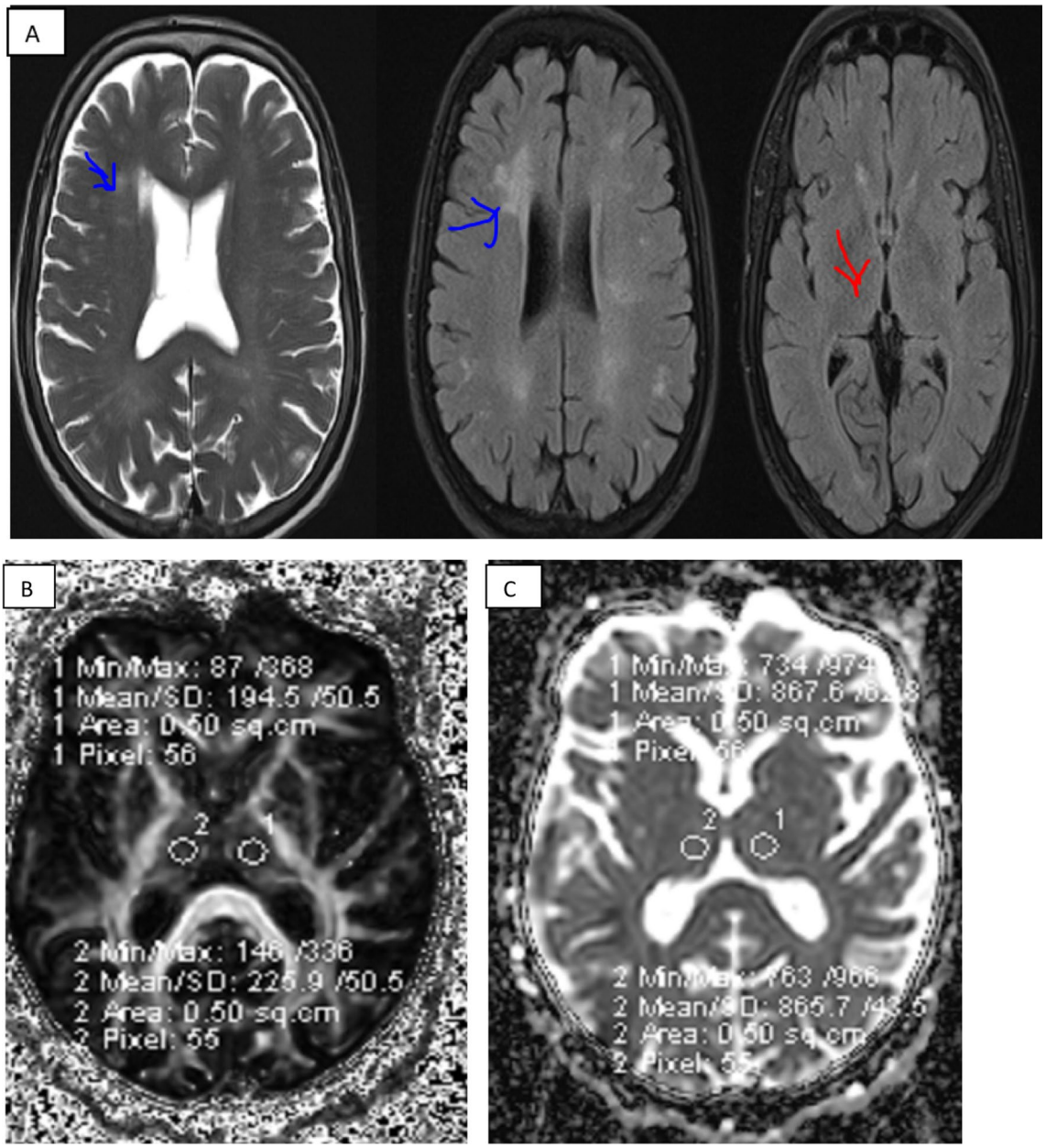

Fig. 8 A 56-year-old female patient complaining of CSVD, image **A** (axial T2 and axial FLAIR) showing periventricular T2 /FLAIR hyper intense lesions (blue arrow) and normal appearing thalami (red arrow). ROI placement in FA images with thalamic value of 226 for the right and 195 for the left one (**B**), ROI placement in ADC images with thalamic value of 866×10^{-6} mm^2/s for the right and 868×10^{-6} mm^2/s for the left one (**C**)

Conclusions

The current study revealed that thalamic DTI and 1H-MRS could detect and discriminate the microstructural changes in normal-appearing thalami in RRMS and CSVD patients. So they can assist in early diagnosis and treatment of these cases, resulting in better prognosis. However, FA in DTI was superior to MRS in discriminating MS and CSVD.

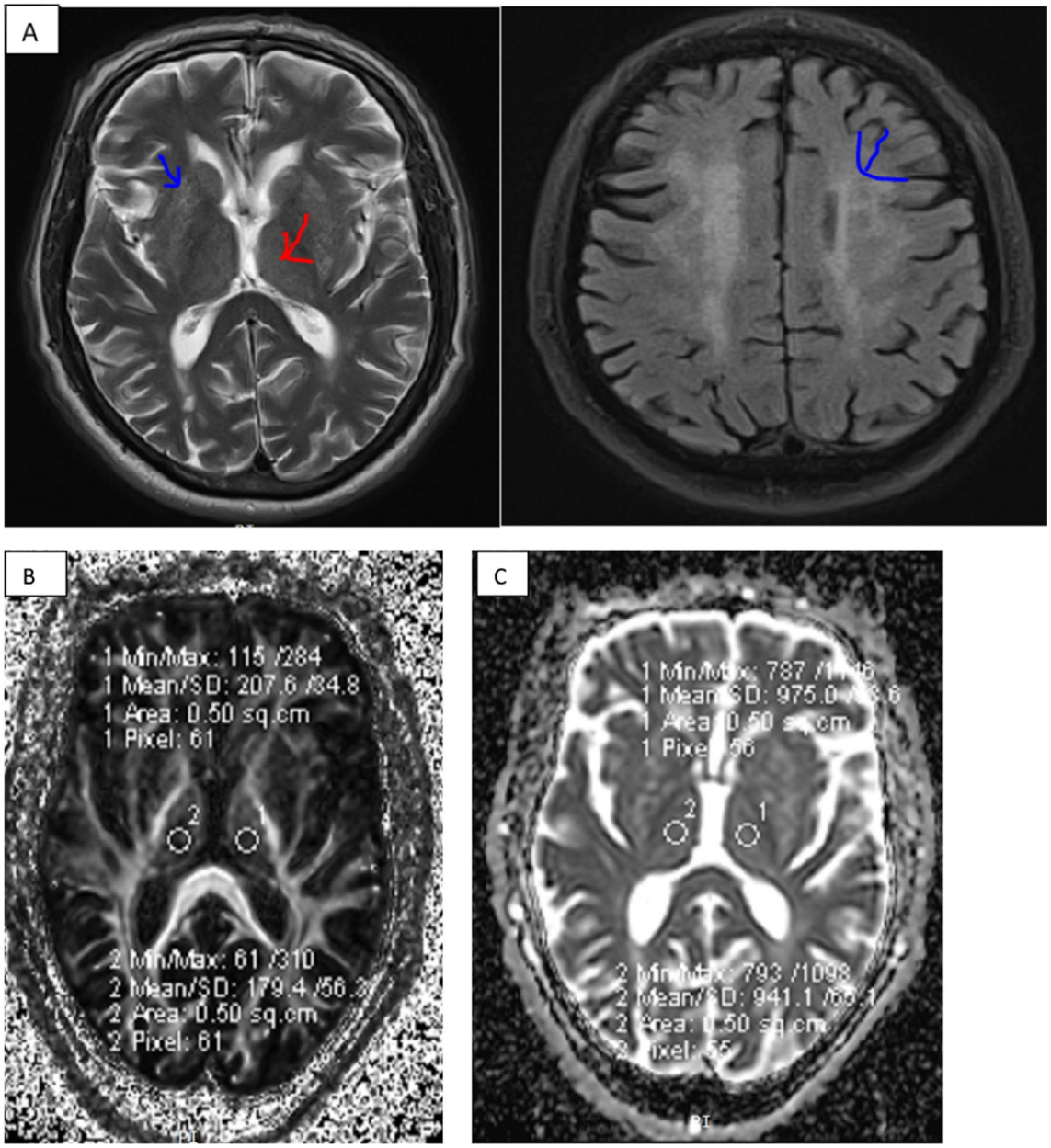

Fig. 9 A 62-year-old male patient complaining of CSVD, image **A** (axial T2 and axial FLAIR) showing periventricular T2 /FLAIR hyper intense lesions (blue arrow) and normal appearing thalami (red arrow). ROI placement in FA images with thalamic value of 179 for the right and 208 for the left one (**B**), ROI placement in ADC images with thalamic value of 941×10^{-6} mm^2/s for the right and 975×10^{-6} mm^2/s for the left one (**C**)

Larger further studies are needed to focus on all MS subtypes. Also, using a d3 Tesla MRI scanner is recommended in the upcoming studies.

Abbreviations

DTI	Diffusion tensor imaging
1H-MRS	Magnetic resonance spectroscopy
MS	Multiple sclerosis
CVSD	Cerebrovascular small vessel disease
FA	Fractional anisotropy
ADC	Apparent diffusion coefficient
Rt	Right
LT	Left
MRI	Magnetic resonance imaging
WM	White matter
CNS	Central nervous system

Acknowledgements
Not applicable.

Author contributions
All authors shared in examination, collection of data of patients and in writing of the manuscript.

Funding
No funding was obtained for this study.

Availability of data and materials
All data are available upon request.

Declarations

Ethics approval and consent to participate
The study was approved by the ethical committee in the Faculty of Medicine, Beni-Suef University (Approval number: FMBSUREC/03012021/Mohamed). Written informed consent was obtained from each participant in this study.

Consent for publication
Consent for publication was obtained from all participants.

Competing interests
"The authors declare that they have no competing interests."

Received: 31 August 2023 Accepted: 30 December 2023
Published online: 08 January 2024

References

1. Wang B, Li X, Li H, Xiao L, Zhou Z, Chen K, Gui L, Hou X, Fan R, Chen K, Wu W, Li H, Hu X (2022) Clinical, radiological and pathological characteristics between cerebral small vessel disease and multiple sclerosis: a review. Front Neurol 13:841521. https://doi.org/10.3389/fneur.2022.841521
2. Cannistraro RJ, Badi M, Eidelman BH, Dickson DW, Middlebrooks EH, Meschia JF (2019) CNS small vessel disease: a clinical review. Neurology 92(24):1146–1156
3. Lie IA, Weeda MM, Mattiesing RM, Mol MAE, Pouwels PJW, Barkhof F, Torkildsen Ø, Bø L, Myhr K-M, Vrenken H (2022) Relationship between white matter lesions and gray matter atrophy in multiple sclerosis. Syst Rev 98(15):e1562–e1573. https://doi.org/10.1212/wnl.0000000000200006
4. Bao J, Tu H, Li Y, Sun J, Hu Z, Zhang F, Li J (2022) Diffusion tensor imaging revealed microstructural changes in normal-appearing white matter regions in relapsing-remitting multiple sclerosis. Front Neurosci 16:837452. https://doi.org/10.3389/fnins.2022.837452
5. Raja R, Rosenberg G, Caprihan A (2019) Review of diffusion MRI studies in chronic white matter diseases. Neurosci Lett 694:198–207. https://doi.org/10.1016/j.neulet.2018.12.007
6. Sun J, Song H, Yang Y, Zhang K, Gao X, Li X, Ni L, Lin P, Niu C (2017) Metabolic changes in normal appearing white matter in multiple sclerosis patients using multivoxel magnetic resonance spectroscopy imaging. Medicine 96(14):e6534. https://doi.org/10.1097/md.0000000000006534
7. Hnilicová P, Štrbák O, Kolisek M, Kurča E, Zeleňák K, Sivák Š, Kantorová E (2020) Current methods of magnetic resonance for noninvasive assessment of molecular aspects of pathoetiology in multiple sclerosis. Int J Mol Sci. https://doi.org/10.3390/ijms21176117
8. ElSayed MEKA, El-Toukhy MMB, Asaad RE, El-Serafy OA (2019) Diffusion tensor imaging for assessment of normally appearing white matter of the brain and spinal cord in cases of multiple sclerosis: a multi-parametric correlation in view of patient's clinical status. Egypt J Radiol Nucl Med 50(1):30. https://doi.org/10.1186/s43055-019-0031-x
9. Tuttle C, Boto J, Martin S, Barnaure I, Korchi AM, Scheffler M, Vargas MI (2019) Neuroimaging of acute and chronic unilateral and bilateral thalamic lesions. Insights Imaging 10(1):24. https://doi.org/10.1186/s13244-019-0700-3
10. Filippi M, Preziosa P, Banwell BL, Barkhof F, Ciccarelli O, De Stefano N, Geurts JJG, Paul F, Reich DS, Toosy AT, Traboulsee A, Wattjes MP, Yousry TA, Gass A, Lubetzki C, Weinshenker BG, Rocca MA (2019) Assessment of lesions on magnetic resonance imaging in multiple sclerosis: practical guidelines. Brain 142(7):1858–1875. https://doi.org/10.1093/brain/awz144
11. Thompson AJ, Banwell BL, Barkhof F, Carroll WM, Coetzee T, Comi G, Correale J, Fazekas F, Filippi M, Freedman MS, Fujihara K, Galetta SL, Hartung HP, Kappos L, Lublin FD, Marrie RA, Miller AE, Miller DH, Montalban X, Mowry EM, Sorensen PS, Tintoré M, Traboulsee AL, Trojano M, Uitdehaag BMJ, Vukusic S, Waubant E, Weinshenker BG, Reingold SC, Cohen JA (2018) Diagnosis of multiple sclerosis: 2017 revisions of the McDonald criteria. Lancet Neurol 17(2):162–173. https://doi.org/10.1016/s1474-4422(17)30470-2
12. Kurtzke JF (2008) Historical and clinical perspectives of the expanded disability status scale. Neuroepidemiology 31(1):1–9. https://doi.org/10.1159/000136645
13. Sparacia G, Agnello F, Gambino A, Sciortino M, Midiri M (2018) Multiple sclerosis: high prevalence of the "central vein" sign in white matter lesions on susceptibility-weighted images. Neuroradiol J 31(4):356–361. https://doi.org/10.1177/1971400918763577
14. Amin M, Ontaneda D (2020) Thalamic injury and cognition in multiple sclerosis. Front Neurol 11:623914. https://doi.org/10.3389/fneur.2020.623914
15. Amiri M, Gerami R, Shekarchi B, Azimi A, Asadi B, Bagheri H (2023) Changes in diffusion tensor imaging indices in basal ganglia and thalamus of patients with relapsing-remitting multiple sclerosis and relation with clinical conditions: a case-control study. Eur J Radiol Open 10:100465. https://doi.org/10.1016/j.ejro.2022.100465
16. Dahshan A, Hassan A, Homos M, Ghoneimy AT (2018) Diffusivity parameters as markers for NAGM involvement and disease progression in MS patients: diffusion tensor imaging study. Mult Scler Relat Disord 26:251. https://doi.org/10.1016/j.msard.2018.10.067
17. Rahmanzadeh R, Lu PJ, Barakovic M, Weigel M, Maggi P, Nguyen TD, Schiavi S, Daducci A, La Rosa F, Schaedelin S, Absinta M (2021) Myelin and axon pathology in multiple sclerosis assessed by myelin water and multi-shell diffusion imaging. Brain 144(6):1684–1696. https://doi.org/10.1093/brain/awab088
18. Lynn JD, Anand C, Arshad M, Homayouni R, Rosenberg DR, Ofen N, Raz N, Stanley JA (2021) Microstructure of human corpus callosum across the lifespan: regional variations in axon caliber, density, and myelin content. Cereb Cortex 31(2):1032–1045. https://doi.org/10.1093/cercor/bhz221
19. Öztoprak B, Öztoprak İ, Topalkara K, Erkoç MF, Şalk İ (2015) Role of thalamic diffusion for disease differentiation between multiple sclerosis and ischemic cerebral small vessel disease. Neuroradiology 57(4):339–347. https://doi.org/10.1007/s00234-014-1479-z
20. Ray L, Iliff JJ, Heys JJ (2019) Analysis of convective and diffusive transport in the brain interstitium. Fluids Barriers CNS 16(1):6. https://doi.org/10.1186/s12987-019-0126-9
21. Swanberg KM, Landheer K, Pitt D, Juchem C (2019) Quantifying the metabolic signature of multiple sclerosis by in vivo proton magnetic resonance spectroscopy: current challenges and future outlook in the translation from proton signal to diagnostic biomarker. Front Neurol. https://doi.org/10.3389/fneur.2019.01173
22. Mostafa MM, Awad EM, Hazzou AM, Elewa MKA, Aziz TTA, Samy DM (2020) Biochemical and structural magnetic resonance imaging in chronic stroke and the relationship with upper extremity motor function. Egypt J Neurol Psychiatry Neurosurg 56(1):50. https://doi.org/10.1186/s41983-020-00183-2
23. Kirov II, Tal A, Babb JS, Herbert J, Gonen O (2013) Serial proton MR spectroscopy of gray and white matter in relapsing-remitting MS. Neurology 80(1):39–46. https://doi.org/10.1212/WNL.0b013e31827b1a8c
24. Lichota A, Szewczyk EM, Gwozdzinski K (2020) Factors affecting the formation and treatment of thrombosis by natural and synthetic compounds. Int J Mol Sci 21(21):7975. https://doi.org/10.3390/ijms21217975
25. Geurts JJG, Reuling IEW, Vrenken H, Uitdehaag BMJ, Polman CH, Castelijns JA, Barkhof F, Pouwels PJW (2006) MR spectroscopic evidence for thalamic and hippocampal, but not cortical, damage in multiple sclerosis. Magn Reson Med 55(3):478–483. https://doi.org/10.1002/mrm.20792
26. Kapeller P, Ropele S, Enzinger C, Lahousen T, Strasser-Fuchs S, Schmidt R, Fazekas F (2005) Discrimination of white matter lesions and multiple sclerosis plaques by short echo quantitative 1H—magnetic resonance spectroscopy. J Neurol 252(10):1229–1234. https://doi.org/10.1007/s00415-005-0847-3

Publisher's Note